The 2013 hot, dry summer in Western Europe

Article

Accepted Version

Dong, B. ORCID: https://orcid.org/0000-0003-0809-7911, Sutton, R. ORCID: https://orcid.org/0000-0001-8345-8583 and Shaffrey, L. ORCID: https://orcid.org/0000-0003-2696-752X (2014) The 2013 hot, dry summer in Western Europe. Bulletin of the American Meteorological Society, 95 (9). S61-S66. ISSN 1520-0477 doi: 10.1175/1520-0477-95.9.S1.1 Available at https://centaur.reading.ac.uk/37054/

www.reading.ac.uk/centaur

THE 2013 HOT, DRY SUMMER IN WESTERN EUROPE

BUWEN DONG, ROWAN SUTTON AND LEN SHAFFREY—National Centre for Atmospheric

Science, Department of Meteorology, University of Reading, Reading, United Kingdom;

7   *Summary*

8   Anthropogenic forcing played a substantial part in Western Europe's hot, dry summer

9   in 2013. North Atlantic sea surface temperatures were likely a factor in the large contrast with

10   summer 2012.

11   *Observations*

12   Western Europe experienced sweltering high temperatures in summer 2013. On 22

13   July 2013, the United Kingdom recorded its hottest day since July 2006, with 33.5°C

14   recorded at Heathrow and Northolt in west London (Met Office 2014). Averaged over

15   Western Europe (Fig 1c), the seasonal mean (June–August) anomaly in surface air

16   temperature (SAT) was 1.33°C above the mean over the period of 1964–93, which is 3.2

17   standard deviations of the interannual variability. [HadCRUT4 data (Morice et al. 2012)

18   shows a similar warming of 1.28°C.] This magnitude of warming is slightly less but

19   comparable with the previous hot summers in Western Europe, such as 2003 (e.g., Schaer et

20   al. 2004) and 2010 (e.g., Barriopedro et al. 2011) for which summer mean SAT anomalies

21   were 1.46°C and 1.86°C respectively, corresponding to 3.5 and 4.5 standard deviations.

22   The atmospheric circulation in summer 2013 was characterized by anomalously high

23   sea level pressure (SLP) extending from the United Kingdom into northern Europe and

24   anomalously low SLP over the Arctic (Fig. 1a). This pattern projects strongly onto the

25   positive phase of the summer North Atlantic Oscillation (SNAO; Folland et al. 2009). The

26   anomalous SNAO index of 2.7 hPa in 2013 was +1.0 standard deviation of the interannual

27   variability, in stark contrast with the previous summer of 2012 for which the index was -2.7

28   standard deviations (Supplementary Fig. S1b). The circulation pattern in 2013 was associated

29   with a northward shift of summer North Atlantic storm track (Fig. 1e and f). The climatology

30   of cyclone track density (Dong et al. 2013a and Fig. 1e) shows a split into two preferred

31   cyclone paths at the North Atlantic jet exit region (5°W–5°E): one passing near Iceland at

~71°N and into the Nordic Seas and the other passing across the British Isles at ~56°N and into Western Europe. In summer 2013, more storms than usual passed over Iceland and fewer over the United Kingdom and into Western Europe (Fig. 1f). This led to dry conditions in the United Kingdom and most of Western Europe. The area-averaged precipitation anomaly was –0.35 mm day^{-1}, which is –2.2 standard deviations of the interannual variability (Supplementary Fig. S1c). The low rainfall was also in stark contrast to the summer of 2012, which was a record wet summer in the United Kingdom and was last in a series of wet UK summers since 2007, each of which was associated with a negative SNAO index (Allan and Folland 2012; Dong et al. 2013b). [Note that the inhomogeneity of the data in E-OBS precipitation is a potential source of bias (Zolina et al. 2014), but negative precipitation anomalies in Western Europe are consistent with the northward shifted storm track.]

Global SST anomalies for summer 2013 are illustrated in Fig. 1d. Warm SSTs (relative to 1964–93) were present in many regions, with a prominent warm anomaly (> 1.0°C) along the Gulf Stream extension in the North Atlantic. Associated with this feature were an enhanced meridional SST gradient to the north and a reduced gradient to the south (Supplementary Fig. S2c). These anomalous SST gradients may have played a role in the observed northward shift of the North Atlantic storm track (e.g., Sampe et al. 2010; Ogawa et al. 2012) and influenced the related anomalies in the SNAO and Western European climate (Folland et al. 2009; Sutton and Dong 2012; Dong et al. 2013a). Warm anomalies were also observed in the Arctic, consistent with the continuing low sea ice extent (SIE); these SIE anomalies might also have had an influence on the atmospheric circulation (Balmaseda et al. 2010; Petrie et al. 2014).

Relative to the climatological period of 1964–93, by 2012 there were significant increases in anthropogenic greenhouse gas (GHG) concentrations (e.g., WMO 2013) and significant changes in anthropogenic aerosols. European and North American sulphur dioxide

57 emissions had declined while Asian emissions had increased (e.g., Lamarque et al. 2010). In

58 this study, we investigate the roles of changes in SST, SIE, and radiative forcing in shaping

59 the European summer of 2013, as well as possible reasons for the striking contrast between

60 summer 2013 and summer 2012. Our focus is on seasonal mean conditions rather than on

61 shorter-lived events that occurred within the season.

62 *Climate model experiments*

63   Climate model experiments have been carried out to identify the roles of changes in:

64 (a) SST/SIE and (b) anthropogenic GHG and aerosol forcing in the European summer climate

65 anomalies of 2013. In this study, we do not address the anthropogenic contribution to the

66 SST/SIE changes, but rather consider these changes as an independent forcing factor. We use

67 the atmosphere configuration of the Met Office Hadley Centre Global Environment Model

68 version 3 (HadGEM3-A; Hewitt et al. 2011), with a resolution of 1.875° longitude by 1.25°

69 latitude and 85 levels in the vertical. Dong et al. (2013b) used the same model to study the

70 2012 summer in Europe. A series of experiments was performed, the details of which are

71 summarized in Table 1. We use the same control experiment (CONTROL) for the period

72 1964–93 as Dong et al. (2013b) and perform two other experiments: ALL2013 and SST2013.

73 Both of these experiments use 2013 SST and SIE boundary conditions but they differ in the

74 specification of anthropogenic GHG and aerosol forcing: ALL2013 uses anthropogenic

75 forcing appropriate for 2013 while SST2013 uses the same anthropogenic forcing as for the

76 CONTROL experiment, appropriate for 1964–93. The last 25 years of each experiment are

77 used for analysis. The CONTROL experiment reproduces realistic climatological SLP and

78 precipitation patterns for summer (Supplemental Fig. S10.2 of Dong et al. 2013b).

79   The model simulates a significant warming over Europe in summer 2013 in response

80 to changes in SST, SIE, and anthropogenic forcing (i.e., ALL2013-CONTROL, Fig. 2a) with

81 an area averaged SAT change of 1.11°C over Western Europe. The observed anomaly of

82   1.33°C is within the ±1 standard deviation range of the interannual variability of the model

83   response (Supplementary Fig. S1a). Changes in SST and SIE explain 63% (±26%) of the

84   area-averaged Western European warming response in HadGEM3 (Fig. 2d), with the

85   remaining 37% (± 29%) explained by the direct impact (without forcing-induced SST and sea

86   ice feedbacks) of changes in radiative forcings from GHG and aerosols (Fig. 2g and

87   Supplementary Fig. S1a).

88   The atmospheric circulation anomalies simulated by the model (Fig. 2b) show notable

89   similarities to the observed pattern over the North Atlantic and Europe (Fig. 1a), including

90   low SLP anomalies over Greenland and an anomalous anticyclone over the United Kingdom.

91   The wave train pattern of SLP anomalies suggests that changes in convection over the

92   Caribbean Sea might be an important factor (e.g., Douville et al. 2011). However, in the

93   model simulation the anomalous anticyclone does not extend as far eastward into central

94   Europe as in the observations. The circulation anomalies correspond to a positive anomaly

95   (mean = 1.2 hPa, which is only 0.5 standard deviations) in the SNAO index relative to the

96   CONTROL, which is smaller than the observed anomaly (2.7 hPa; Supplementary Fig. S1b).

97   The pattern of simulated Western European precipitation anomalies (Fig. 2c) is consistent

98   with the positive phase of the SNAO and is similar to the observations, with anomalously low

99   rainfall over most of Western Europe (Fig. 1b). As for the circulation anomaly, the magnitude

100 of the mean precipitation anomaly is smaller than observed (Supplementary Fig S1c),

101 although there is substantial interannual variability in the model results.

102   The additional SST2013 experiment suggests that *both* SST/SIE changes and the

103 direct impact of changes in anthropogenic radiative forcing contributed to the anomalous

104 circulation (Figs. 2e and h, Fig. S1b) and reduced rainfall over Western Europe in summer

105 2013 (Figs. 2f and i; Supplementary Fig. S1c). The SST change has the most impact on the

106 low SLP anomalies simulated over Greenland, but GHG and aerosol forcing causes a

substantial anticyclonic anomaly over, and north of, the United Kingdom. This anticyclonic circulation anomaly is similar to the summer mean circulation response to an increase in GHG forcing (Blade et al. 2012) and is presumably due to an increase in the frequency of the positive SNAO-like circulation regimes over the Atlantic sector (Boe et al. 2009).

Changes in GHG and aerosol forcing are unlikely to be a major factor in explaining the striking contrast in circulation and precipitation between the European summers of 2012 and 2013 (Supplementary Fig. S2a), as the changes in these forcings between these two years were small. However, the model experiments suggest that changes in SST and SIE in the North Atlantic were a significant factor (Supplementary Fig. S2e). In particular, the anomalous meridional SST gradient to the north of the Gulf Stream in 2013, relative to 2012 (Supplementary Fig. S2c), may have favored a positive phase of the SNAO and a northward shift of North Atlantic summer storm track (e.g., Folland et al. 2009; Dong et al. 2013a), as was observed (Supplementary Figs. S2d and f). The model experiments show some evidence of capturing this shift, although the mean signal (Supplementary Fig. S2e) is again much weaker than was observed (Supplementary Fig. S2a).

The model results show an encouraging degree of consistency with observations, but it is difficult to assess precisely what level of consistency should be expected in view of the high level of internal variability and uncertainty about the true magnitude of forced signals in the real world. It is clear from Supplementary Fig. S1 that the signal-to-noise ratio for the changes in SAT is large, which permits more confident conclusions, whereas that for changes in circulation and precipitation is much lower (though it is interesting to note that the model suggests a stronger forced signal in Western European summer precipitation than in the SNAO). One limitation of the current experiments, which may well influence the signal-to-noise ratio, is the use of a prescribed SST boundary condition. Active ocean–atmosphere coupling may modify the response to forcings and is an important area of future work (Sutton

132   and Mathieu 2002; Dong et al. 2013a). Another extension not addressed here is the

133   anthropogenic contribution to the SST/SIE changes.

134   *Conclusions*

135   The European summer of 2013 was marked by hot and dry conditions in Western

136   Europe associated with a northward shifted Atlantic storm track and a positive phase of the

137   SNAO. Model results suggest that, relative to a 1964–93 reference period, changes in

138   SST/SIE explain 63% ($\pm26\%$) of the area-averaged warming signal over Western Europe,

139   with the remaining 37% ($\pm29\%$) explained by the direct impact of changes in anthropogenic

140   radiative forcings from GHG and aerosols. The results further suggest that the anomalous

141   atmospheric circulation, and associated low rainfall, were also influenced both by changes in

142   SST/SIE and by the direct impact of changes in radiative forcings; however, the magnitude of

143   the forced signals in these variables is much less, relative to internal variability, than for

144   surface air temperature. Further evidence suggests that changes in North Atlantic SST were

145   likely an important factor in explaining the striking contrast between the European summers

146   of 2013 and that of 2012. A major area for further work is to understand more completely the

147   mechanisms that explain these influences.

148

149

150   **REFERENCES:**

151   Allan, R., and C. K. Folland, 2012: [Global climate] Atmospheric circulation: Mean sea level
152   pressure. [In "State of the Climate 2011"]. *Bull. Amer. Meteor. Soc.*, **93** (7), S35–S36.

153   Barriopedro, D., E. M. Fischer, J. Lutenbacher, R. M. Trigo, and R. Garcia-Herrera, 2011:
154   The hot summer of 2010: redrawing the temperature record map of Europe. *Science*,
155   **332**, 220–224.

156   Balmaseda, M. A., L. Ferranti, F. Molteni, and T. N. Palmer, 2010: Impact of 2007 and 2008
157   Arctic ice anomalies on the atmospheric circulation: Implications for long-range
158   predictions. *Quart. J. Roy. Meteor. Soc.*, **136**, 1655–1664.

159   Boé, J., L. Terray, C. Cassou and J. Najac, 2009: Uncertainties in European summer
160   precipitation changes: role of large scale circulation. *Clim. Dyn.,* **33**, 265–276. doi:10.
161   1007/s00382-008-0474-7.

162   Bladé, I., B. Liebmann, D. Fortuny, and G. J. Oldenborgh, 2012: Observed and simulated
163   impacts of the summer NAO in Europe: Implications for projected drying in the
164   Mediterranean region, *Clim. Dyn.*, **39**, 709–727, doi:10.1007/s00382-011-1195-x.

165   Dong, B., R. T. Sutton, T. Woollings, and K. Hodges, 2013a: Variability of the North
166   Atlantic summer stormtrack: Mechanisms and impacts. *Environ. Res. Lett.*, **8**, 034037
167   doi:10.1088/1748-9326/8/3/034037

168   Dong, B.-W., R. T. Sutton, and T. Woollings, 2013b: The extreme European summer 2012
169   (in "Explaining Extreme Events of 2012 from a Climate Perspective"). *Bull. Amer.*
170   *Meteor. Soc.,* **94** (9), S28–S32.

171   Douville, H., S. Bielli, C. Cassou, M. Dequé, N. M. J. Hall, S. Tyteca, and A. Voldoire, 2011:
172   Tropical influence on boreal summer mid-latitude stationary waves. *Climate Dyn.*, **38**,
173   1783–1798.

174   Folland, C. K., J. Knight, H. W. Linderholm, D. Fereday, S. Ineson, and J. W. Hurrell, 2009:
175   The summer North Atlantic oscillation: Past, present, and future. *J. Climate*, **22**,
176   1082–1103.

177   Haylock, M. R., N. Hofstra, A. M. G. Klein Tank, E. J. Klok, P. D. Jones, and M. New, 2008:
178   A European daily high-resolution gridded dataset of surface temperature and
179   precipitation for 1950–2006. *J. Geophys. Res.*, **113**, D20119,
180   doi:10.1029/2008JD010201.

181   Hewitt, H. T., D. Copsey, I. D. Culverwell, C. M. Harris, R. S. R. Hill, A. B. Keen, A. J.
182   McLaren, and E. C. Hunke, 2011: Design and implementation of the infrastructure of
183   HadGEM3: The next-generation Met Office climate modelling system. *Geosci. Model*
184   *Dev.*, **4**, 223–253.

185 Hoskins, B. J., and K. I. Hodges, 2002: New perspectives on the Northern Hemisphere winter
186   storm tracks. *J. Atmos. Sci.,* **59**, 1041–1061.

187 Kalnay, E., and Coauthors, 1996: The NCEP-NCAR 40-year reanalysis project. *Bull. Amer.*
188   *Meteor. Soc.,* **77**, 437–471.

189 Lamarque, J.-F.*,* and Coauthors, 2010: Historical (1850–2000) gridded anthropogenic and
190   biomass burning emissions of reactive gases and aerosols: Methodology and
191   application. *Atmos. Chem. Phys.,* **10***,* 7017–7039, doi:10.5194/acp-10-7017-2010.

192 Met Office, cited 2014: Hot dry spell July 2013. [Available online at
193   http://www.metoffice.gov.uk/climate/uk/interesting/2013-heatwave.]

194 Morice, C. P., J. J. Kennedy, N. A. Rayner, and P. D. Jones, 2012: Quantifying uncertainties
195   in global and regional temperature change using an ensemble of observational
196   estimates: The HadCRUT4 dataset, *J. Geophys. Res.*, **117,** D08101,
197   doi:10.1029/2011JD017187.

198 Ogawa, F., H. Nakamura, K. Nishii, T. Miyasaka, and A. Kuwano-Yoshida, 2012:
199   Dependence of the climatological axial latitudes of the tropospheric westerlies and
200   storm tracks on the latitude of an extratropical oceanic front. *Geophys. Res. Lett.*,
201   doi:10.1029/2011GL049922

202 Petrie, R., L. C. Shaffrey, and R. T. Sutton, 2014: The atmospheric response to Arctic sea ice
203   decline. *Geophy. Res. Lett.,* (submitted).

204 Rayner, N. A., D. E. Parker, E. B. Horton, C. K. Folland, L. V. Alexander, D. P. Rowell, E.
205   C. Kent, and A. Kaplan, 2003: Global analyses of sea surface temperature, sea ice,
206   and night marine air temperature since the late nineteenth century. *J. Geophys. Res.,*
207   **108** (D14), 4407, doi:10.1029/2002JD002670.

208 Sampe, T., H. Nakamura, A. Goto, and W. Ohfuchi, 2010: Significance of a midlatitude SST
209   frontal zone in the formation of a storm track and an eddy-driven westerly jet. *J.*
210   *Climate*, **23**, 1793–1814.

211 Schaer, C., P. L. Vidale, D. Luethi, C. Frei, C. Haeberli, M. A. Liniger and C. Appenzeller,
212   2004: The role of increasing temperature variability in European summer heatwaves.
213   *Nature,* **427,** 332–336.

214 Sutton, R. T., and B.-W. Dong, 2012: Atlantic Ocean influence on a shift in European climate
215   in the 1990s. *Nature Geosci.*, **5**, 788–792, doi:10.1038/ngeo1595.

216 Sutton, R. T., and P.P. Mathieu, 2002: Response of the atmosphere–ocean mixed-layer
217   system to anomalous ocean heat-flux convergence. *Quart. J. Roy. Meteor. Soc.*, **128**,
218   1259–1275

219 WMO, 2013: The state of greenhouse gases in the atmosphere based on global observations
220   through 2012. *WMO Greenhouse Gas Bulletin*, No. 9, 4 pp.

221   Zolina, O., and Coauthors, 2014: New view on precipitation variability and extremes in
222   Central Europe from a German high resolution daily precipitation dataset: Results
223   from STAMMEX project *Bull. Am. Meteorol. Soc.* at press (doi:10.1175/BAMS-D-
224   12-00134.1)

225

226   **Table 1.** Summary of numerical experiments.

Experiments	Boundary conditions	Length of run
CONTROL	Forced with monthly mean climatological sea surface temperature (SST) and sea ice extent (SIE) averaged over the period of 1964 to 1993 using HadISST data (Rayner et al. 2003) and with anthropogenic greenhouse gases (GHG) concentrations averaged over the same period and anthropogenic aerosols emissions averaged over the period of 1970 to 1993.	32 years
ALL2013	Forced with monthly mean SST and SIE from December 2012 to November 2013 using HadISST data, with anthropogenic GHG concentration in 2012 (WMO 2013) and anthropogenic aerosol emissions for 2010 (Lamarque et al. 2010), which is the most recent year for which emissions data were available.	27 years
SST2013	As ALL2013, but with anthropogenic GHG concentrations and anthropogenic aerosol emissions the same as in CONTROL.	27 years

227

228

Figure legends

FIGURE. 1. Anomalies for JJA 2013 from the climatological period 1964-1993 for (a) SLP (hPa) and (c) SAT (^{o}C) from NCEP reanalysis (Kalnay et al. 1996), (b) percentage precipitation change (%) from the daily gridded E-OBS precipitation (version 9.0) over Europe (Haylock et al. 2008) and (d) SSTs (^{o}C) from HadISST (Rayner et al. 2003). (e) and (h) for the climatological period and 2013 cyclone track density as in Hoskins and Hodges (2002) based on NCEP reanalysis. Track density is in unit of numbers per month per unit area, where the unit area is equivalent to a 5° spherical cap (about 10^{6} km^{2}). Note that this climatological period is dominated by cold AMO conditions and is the period used for the climatological model simulations. Thick lines in (a) and (c) highlight regions where the differences are statistically significant at the 90% confidence level using a two-tailed Student t-test.

FIGURE. 2. SAT (^{o}C) (left column), SLP (hPa) (middle column) and precipitation changes (right column) (%) in the model simulations forced by different configurations of forcings in 2013 relative to the control simulation. (a), (b) and (c) forced by changes in SST and SIE, GHG concentrations, and aerosols emissions (ALL2013-CONTROL). (d), (e) and (f) forced by changes in SST and SIE (SST2013-CONTROL). (g), h) and (i) forced by changes in GHG and aerosols emissions (ALL2013-SST2013). Only changes that are statistically significant at the 90% confidence level using a two-tailed Student t-test are plotted in (a), (d) and (g) while thick lines in other panels highlight regions where the differences are statistically significant at the 90% confidence level.
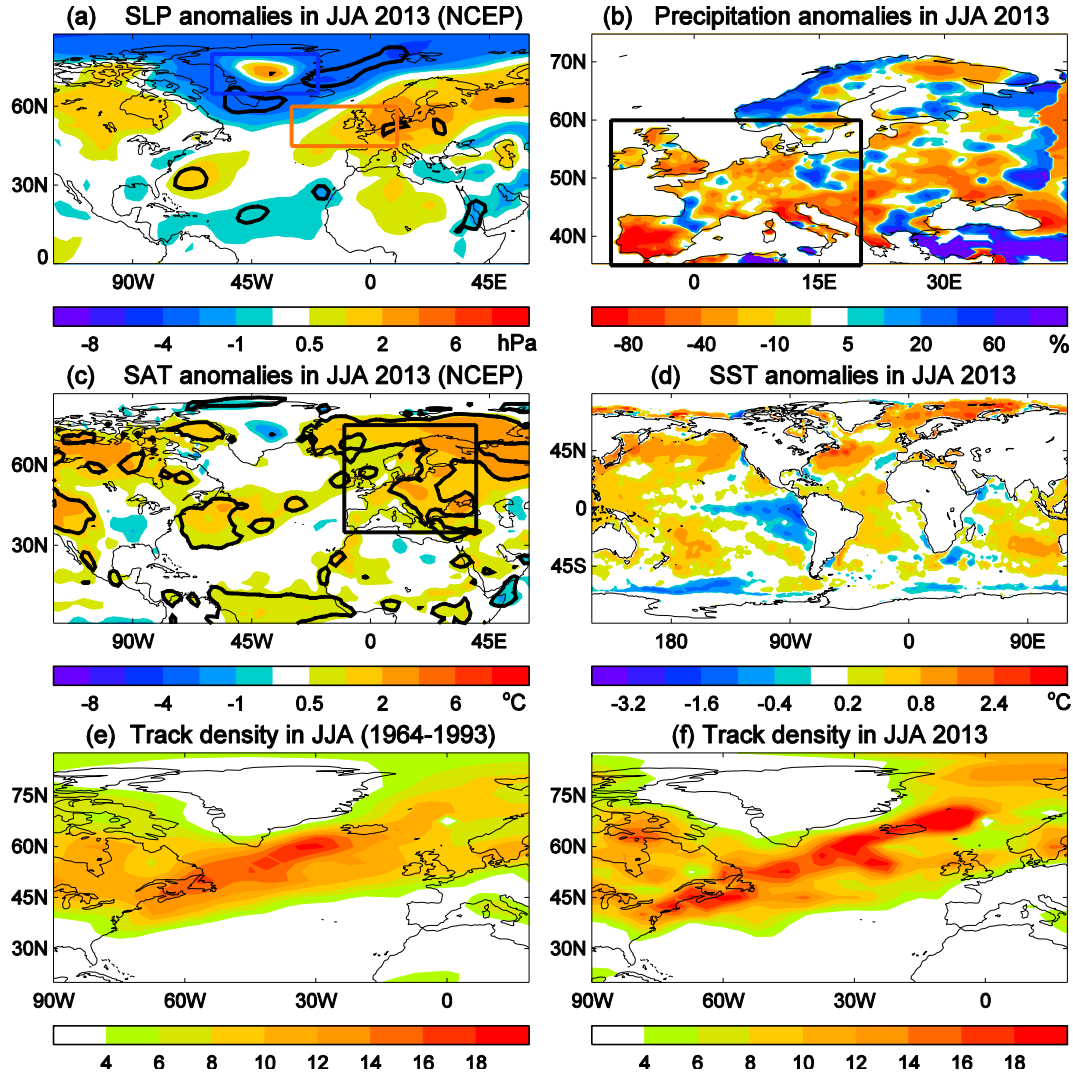
FIGURE. 1. Anomalies for JJA 2013 from the climatological period 1964-1993 for (a) SLP (hPa) and (c) SAT (^{o}C) from NCEP reanalysis (Kalnay et al. 1996), (b) percentage precipitation change (%) from the daily gridded E-OBS precipitation (version 9.0) over Europe (Haylock et al. 2008) and (d) SSTs (^{o}C) from HadISST (Rayner et al. 2003). (e) and (h) for the climatological period and 2013 cyclone track density as in Hoskins and Hodges (2002) based on NCEP reanalysis. Track density is in unit of numbers per month per unit area, where the unit area is equivalent to a 5° spherical cap (about 10^{6} km^{2}). Note that this climatological period is dominated by cold AMO conditions and is the period used for the climatological model simulations. Thick lines in (a) and (c) highlight regions where the differences are statistically significant at the 90% confidence level using a two-tailed Student t-test.
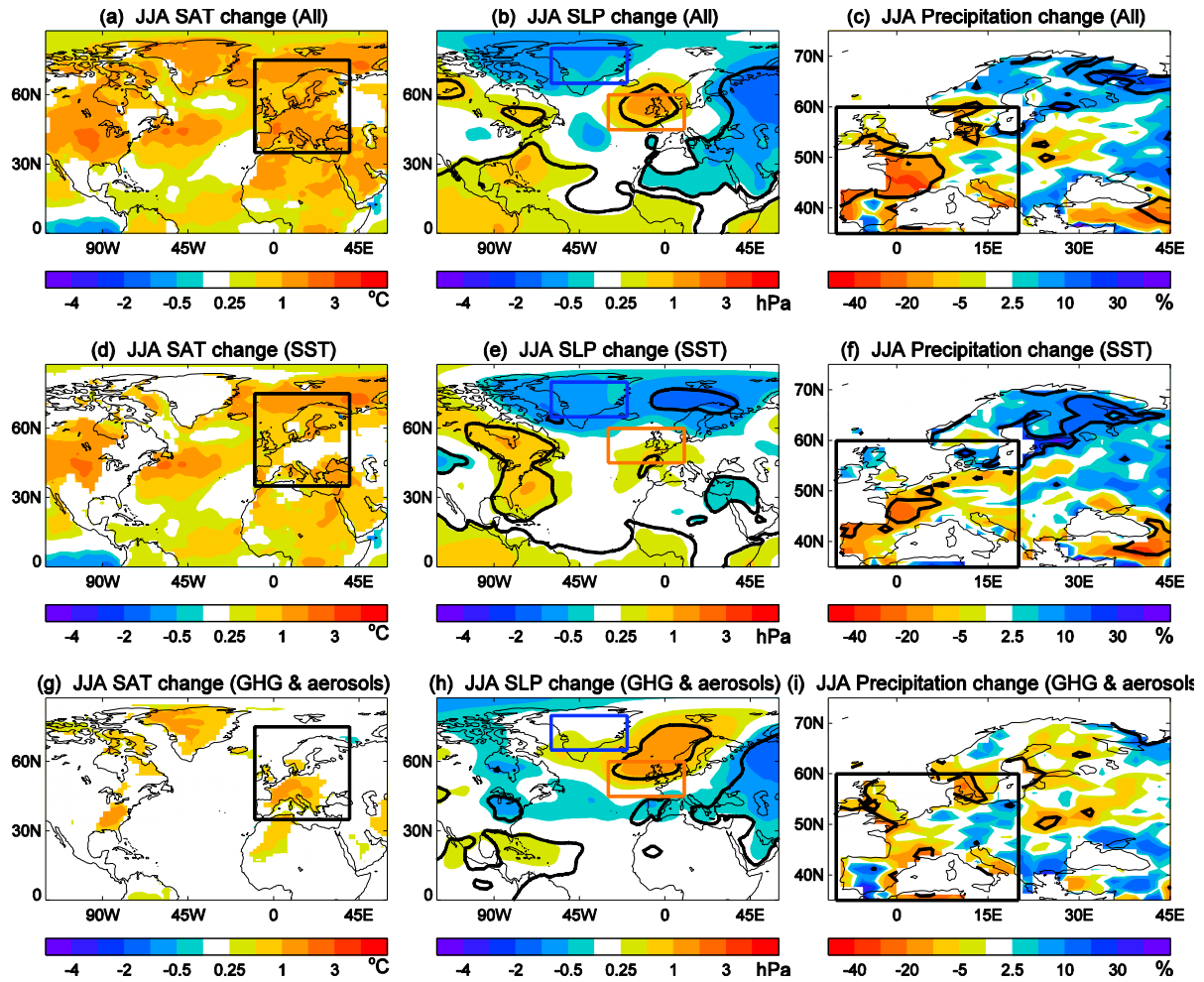
FIGURE. 2. SAT (^{o}C) (left column), SLP (hPa) (middle column) and precipitation changes (right column) (%) in the model simulations forced by different configurations of forcings in 2013 relative to the control simulation. (a), (b) and (c) forced by changes in SST and SIE, GHG concentrations, and aerosols emissions (ALL2013-CONTROL). (d), (e) and (f) forced by changes in SST and SIE (SST2013-CONTROL). (g), h) and (i) forced by changes in GHG and aerosols emissions (ALL2013-SST2013). Only changes that are statistically significant at the 90% confidence level using a two-tailed Student t-test are plotted in (a), (d) and (g) while thick lines in other panels highlight regions where the differences are statistically significant at the 90% confidence level.

SUPPLEMENTAL MATERIALS: THE 2013 HOT, DRY SUMMER IN WESTERN EUROPE
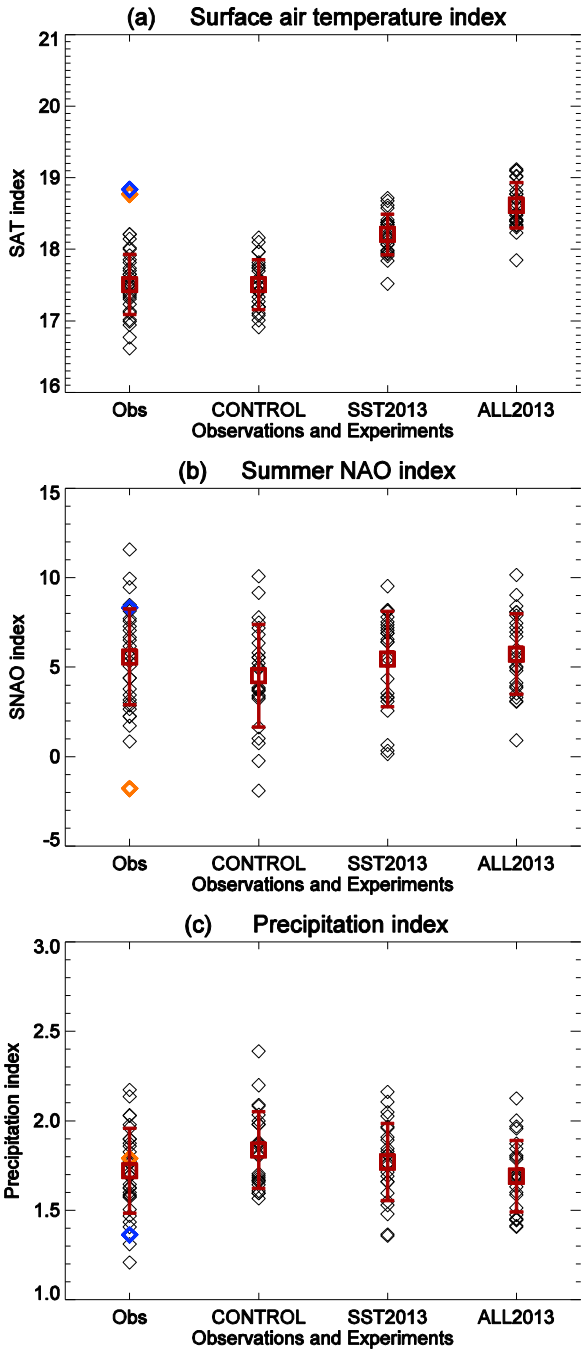
Buwen Dong, Rowan Sutton and Len Shaffrey

Figure S1: (a) SAT (^{o}C), (b) summer NAO (hPa), and (c) precipitation (mm day^{-1}) indices for observations and model experiments. SAT index is area averaged SAT over region (35°N-75°N, 10°W-40°E, land only) (black box in Fig.1c). The SNAO index is defined as the difference of the area mean SLP between two regions around the British Isles (45°-60°N, 30°W-10°E) and over Greenland (65°N-80°N, 60°W-20°W) (red and blue boxes in Fig. 1a). Precipitation index is area averaged precipitation over region (35°N-60°N, 10°W-20°E, land only) (black box in Fig.1b). All black diamonds in observations are for years from 1964 to 1993 with red diamonds for 2012 and blue diamonds for 2013. Red squares and lines are the mean and mean ± sigma ranges where sigma is the corresponding standard deviation.
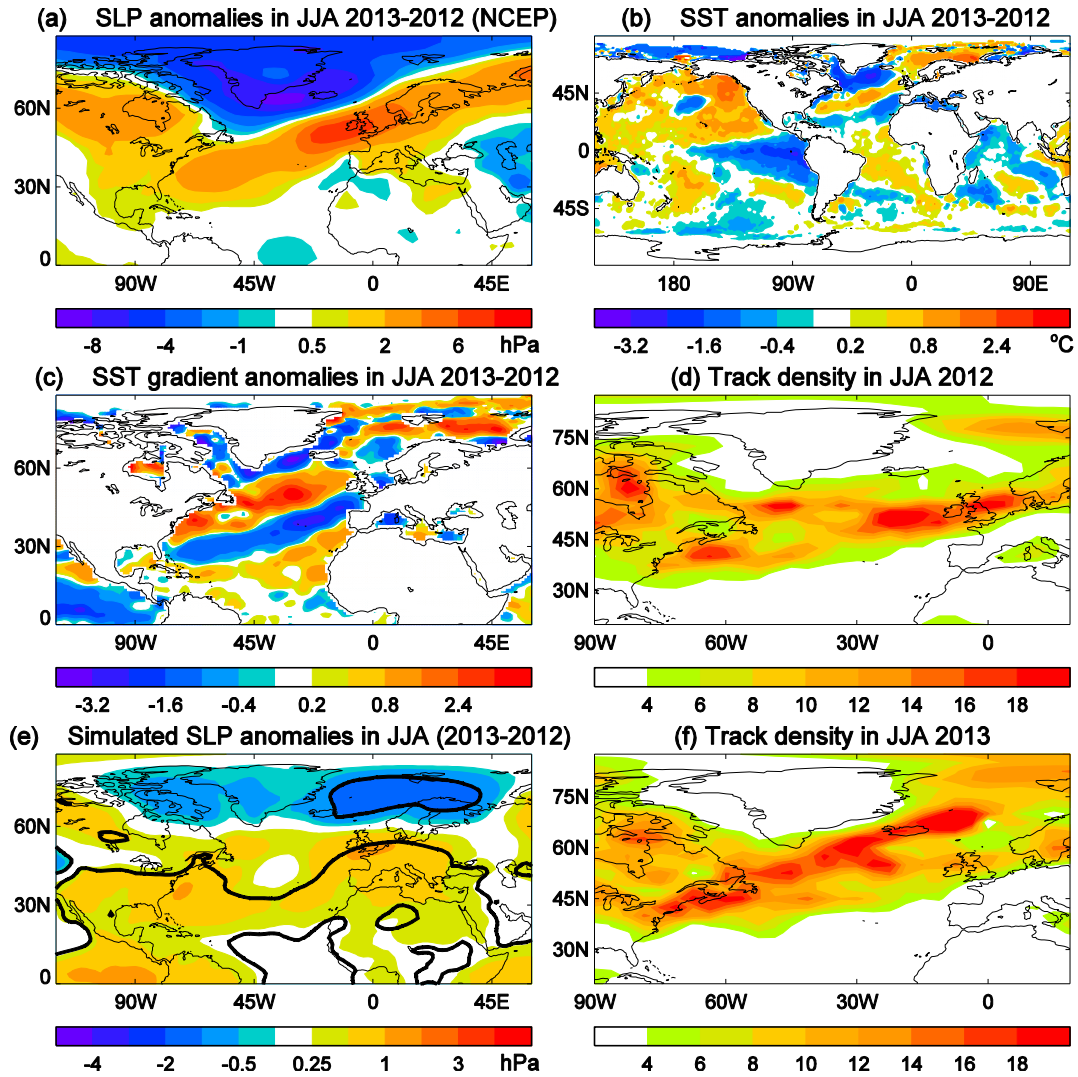
Figure S2. Anomalies in JJA between 2013 and 2012. (a) SLP (hPa), (b) SST (^{o}C), and (c) SST gradient (^{o}C per 1000 km) in observations. (e) Simulated SLP difference between 2013 and 2012 from the changes in SST and SIE. The experiment of 2012 was documented in Dong et al. (2013b). (d) and (f) are 2012 and 2013 cyclone track density. Track density is in unit of numbers per month per unit area, where the unit area is equivalent to a 5° spherical cap (about 10^6 km^2). Note that this climatological period is dominated by cold AMO conditions and is the period used for the climatological model simulations. Thick lines in (e) highlight regions where the differences are statistically significant at the 90% confidence level using a two-tailed Student t-test.